Brief Communication

Neuro–degenerative Diseases

Neurodegener Dis 2016;16:118–124
DOI: 10.1159/000441421

Received: July 6, 2015
Accepted after revision: October 1, 2015
Published online: December 8, 2015

PET Radioligands Reveal the Basis of Dementia in Parkinson's Disease and Dementia with Lewy Bodies

Stephen N. Gomperts[a] Marta Marquie[a] Joseph J. Locascio[a] Stephen Bayer[a]
Keith A. Johnson[a, b] John H. Growdon[a]

Departments of [a]Neurology and [b]Radiology, Massachusetts General Hospital, Boston, Mass., USA

Key Words
Amyloid · Cognitive impairment · Dementia · Dementia with Lewy bodies · Dopamine transporter · Dopaminergic neurons · Neuroimaging · Parkinson's disease · Positron emission tomography · Tau protein

Abstract
Background: Effective therapies for dementia with Lewy bodies (DLB) and Parkinson's disease (PD) dementia will require accurate diagnosis and an understanding of the contribution of distinct molecular pathologies to these diseases. We seek to use imaging biomarkers to improve diagnostic accuracy and to clarify the contribution of molecular species to cognitive impairment in DLB and PD. ***Summary:*** We have performed cross-sectional and prospective cohort studies in subjects with DLB, PD with normal cognition, PD with mild cognitive impairment and PD with dementia, contrasted with Alzheimer's disease (AD) and healthy control subjects (HCS). Subjects underwent formal neurological examination, detailed neuropsychological assessments, MRI and PET scans with the radioligands altropane (a dopamine transporter, DAT) and Pittsburgh compound B (PiB; β-amyloid). Putamen DAT concentrations were similar in DLB and PD and differentiated them from HCS and AD. Decreased caudate DAT concentration related to functional impairment in DLB but not PD. PiB uptake was greatest in DLB. However, cortical PiB retention was common in PD and predicted cognitive decline. PET imaging of tau aggregates holds promise both to clarify the contribution of tau to cognitive decline in these diseases and to differentiate DLB and PD from the parkinsonian tauopathies. ***Key Messages:*** Together, DAT and amyloid PET imaging discriminate DLB from PD and from other disease groups and identify pathological processes that contribute to their course. Multimodal PET imaging has the potential to increase the diagnostic accuracy of DLB and PD in the clinic, improve cohort uniformity for clinical trials, and serve as biomarkers for targeted molecular therapies.

Dementia with Lewy bodies (DLB) is the second most common dementia after Alzheimer's disease (AD) [1]. Its clinical features, which include dementia associated with the motor manifestations of parkinsonism, visual hallucinations and fluctuations of cognition, overlap significantly with the clinical features that arise in the context of

KARGER

1660–2854/15/0162–0118$39.50/0

E-Mail karger@karger.com
www.karger.com/ndd

Dr. Stephen N. Gomperts
Department of Neurology, Massachusetts General Hospital
114 16th Street, Room 2004
Charlestown, MA 02129 (USA)
E-Mail sgomperts@partners.org

dementia in idiopathic Parkinson's disease (PD) [2]. DLB and PD dementia (PDD) are differentiated by the relative timing of dementia and parkinsonism, with PDD arising in the context of well-established idiopathic PD, after at least 1 year of motor symptoms, whereas an early onset of dementia is more consistent with a diagnosis of DLB [1]. Both DLB and PDD are characterized neuropathologically by the accumulation of α-synuclein aggregates in Lewy bodies and Lewy neurites in the brain, with cortical Lewy bodies required for a neuropathological diagnosis of DLB but common in PDD. Given their clinical and neuropathological similarities, DLB, PDD and PD have been aggregated conceptually under the broad umbrella of Lewy body disease [2].

Despite the value of the DLB Consortium criteria [1], the accuracy of a clinical diagnosis of DLB remains low. Sensitivity of the DLB consensus criteria has been found to be quite variable, ranging from 12 to 88% across different academic centers [3], and is greatest with inclusion of supportive diagnostic features, including PET imaging demonstrating dopamine cell loss, neuroleptic sensitivity or REM sleep behavioral disorder. In contrast, the specificity of the criteria is higher, ranging from 79 to 100%. The repercussions of an incorrect diagnosis are significant, including risk for neuroleptic exposure, lost opportunity for treatment, and inappropriate exclusion from and inclusion in clinical trials.

Molecular imaging tools hold promise for improving the diagnostic accuracy of DLB. For example, dopamine transporter (DAT) imaging with SPECT or PET can confirm neurodegenerative parkinsonism [4]. Using [^{11}C]altropane, a DAT ligand with selective affinity for the DAT over the norepinephrine transporter or the serotonin transporter (7 nmol affinity, 25-fold greater affinity for the DAT over the serotonin transporter) [5], we have begun to explore the relation of DAT levels with clinical features of DLB and PD [6].

In addition, comorbid AD pathology is common in DLB, such that approximately 85% of cases contain abundant amyloid plaques [7, 8]. Aggregates of tau in the form of neurofibrillary tangles are also observed [8]. The development of PET ligands that label brain amyloid, such as [^{11}C]Pittsburgh compound B ([^{11}C]PiB), has provided a noninvasive method to explore the contribution of amyloid deposition during life to the clinical features and clinical course of DLB and PD [9]. Amyloid imaging reliably labels fibrillar forms of β-amyloid, including cored plaques, some diffuse plaques and amyloid angiopathy. As negative scans are exceedingly rare in AD, this has proven to be a valuable molecular imaging tool. The clinical relevance of concomitant AD pathology in DLB remains a topic of active investigation. Some studies have found that amyloid deposition impacts the clinical phenotype [10]. In addition, we and other groups have found that amyloid deposition hastens cognitive decline in PD [11, 12].

Recently, several PET ligands have been developed to image paired helical filaments of tau [13], which accumulate in neurofibrillary tangles in AD. One such agent, [^{18}F]T807, has a very high affinity for paired helical filaments of tau and a selectivity for tau over β-amyloid of >27-fold [14]. The application of [^{18}F]T807 imaging to PD and DLB provides a powerful new method to evaluate, during life, the contribution of paired helical filaments of tau to cognitive impairment and clinical phenotype. In addition, to the extent that [^{18}F]T807 may bind tau aggregates in the parkinsonian tauopathies, progressive supranuclear palsy (PSP) and cortical basal ganglionic degeneration, [^{18}F]T807 also has the potential to discriminate between parkinsonian diseases of synuclein and tau.

Here, we report our experience with DAT imaging and amyloid imaging in cross-sectional and longitudinal studies of DLB and PD, as well as our early experience with [^{18}F]T807 PET imaging.

Methods

Subjects

Subjects were recruited from the Massachusetts General Hospital Movement Disorders and Memory Disorders Units and gave informed consent to participate in this research study according to the protocol approved by the Partners Health Care Inc. Institutional Review Board. PD subjects fulfilled criteria for a diagnosis of idiopathic PD according to the UK Parkinson Disease Society Brain Bank Research Center's clinical diagnostic criteria [15]. Criteria for PD with mild cognitive impairment (PD-MCI) were consistent with those of the Movement Disorder Society [16], requiring a cognitive complaint, such as impairment of short-term memory, plus at least one cognitive test score that fell in the impaired range. We used the Movement Disorder Society criteria for PDD [17] and the DLB Consortium consensus criteria for DLB [1]. Each subject underwent standardized neurological examination, cognitive testing and PET imaging.

Clinical Evaluation

Functional status was assessed by the Clinical Dementia Rating Scale Sum of Boxes (CDR-SB). Neuropsychological testing was also acquired, as described in Gomperts et al. [11]. Motor function was assessed with the Hoehn and Yahr stage and the motor subscale of the Unified Parkinson Disease Rating Scale.

For DAT imaging, we enrolled 81 subjects, including 29 with PD without dementia (20 cognitively normal, 9 PD-MCI), 12

DLB, 10 PDD and 6 AD. Twenty-four subjects served as a healthy control subject (HCS) group. Of this cohort, 19 PD, 10 DLB and 17 HCS also underwent structural brain MRI for Freesurfer-derived partial volume correction of PET data. Detailed altropane PET methods are described in Marquie et al. [6].

For PiB imaging, we studied a total of 74 subjects, including 29 PD with normal cognition (PD-nl), 14 PD-MCI, 12 PDD and 18 DLB. Of these, 20 PD-nl, 5 PD-MCI, 10 PDD and 9 DLB had also been imaged with altropane. Data from these subjects were compared with those of a separately collected cohort of 85 HCS. Detailed cross-sectional PiB PET methods are described in Gomperts et al. [18].

All HCS subjects had a normal neurological examination, a CDR-SB score of 0 and normal cognition, with the Blessed Dementia Scale IMC score <3 or Mini Mental State Examination score >27.

For the prospective cohort study, 46 nondemented PD subjects underwent PiB imaging and were then followed with annual cognitive and neurological evaluations, for a mean of 3.9 ± 1.9 visits (range: 1–7 visits). Of the 46 subjects, 35 scored in normal ranges on a set of cognitive tests at study baseline, and 32 of these had no cognitive complaint. Eleven met Movement Disorder Society criteria for MCI [16]. PD-MCI subjects had a global CDR score of at least 0.5. Eight out of 11 cases were amnestic, multidomain MCI, and 3/11 were nonamnestic, multidomain MCI. The memory box score was at least 0.5 in 10 of these subjects. The mean Mini Mental State Examination score was 29.1 ± 1.0 for the PD-nl group and 26.3 ± 2.9 for the PD-MCI group. Detailed longitudinal PiB PET methods are described in Gomperts et al. [11].

We have also acquired [^{18}F]T807 PET imaging in a small number of PiB-imaged subjects with PD, PD-MCI, PDD, DLB, PSP and corticobasal syndrome.

PET Imaging Acquisition and Analyses

[^{11}C]Altropane. Altropane PET images were acquired as described previously [6]. Briefly, 15 mCi [^{11}C]altropane was injected as a bolus and followed with a 60-min dynamic acquisition. DAT concentration was estimated with specific binding of altropane, which was computed in regions of interest (ROIs) using the standardized uptake value ratio (SUVR) [19], a ratio of uptake in the target ROI to reference region measured between 40 and 60 min after injection. The pericalcarine (visual) cortex was selected as reference on the basis of its low DAT concentration [20] and low altropane binding [5]. For caudate ROI analyses, a magnetization-prepared rapid acquisition gradient echo sequence optimized for use with Freesurfer software was acquired to generate high-resolution anatomic data. SUVR images were coregistered to the magnetization-prepared rapid acquisition gradient echo data, and PET data were spatially normalized to the MNI template brain using Statistical Parametric Mapping (SPM2). To compensate for the dilutional effect resulting from the low spatial resolution of PET, partial volume correction was applied to the altropane SUVR using the correction factor derived from the convolved binary brain mask (two-component Meltzer method) as described previously [21].

[^{11}C]PiB. PiB PET images were acquired as previously described [11, 18]. Briefly, 15 mCi of [^{11}C]PiB was injected as a bolus, followed immediately by a 60-min dynamic acquisition phase. Precuneus PiB retention was calculated using the Logan graphical analysis method [22, 23], with cerebellar cortex as the reference tissue input function; specific PiB retention was expressed as the distribution volume ratio (DVR).

[^{18}F]T807 PET Imaging

For [^{18}F]T807 data acquisition, administration of 10 mCi of radiotracer was followed by a 20-min acquisition, beginning at 80 min after injection. We expressed [^{18}F]T807 data as the SUVR with cerebellar reference, as previously reported [14]. SUVR images were coregistered to a magnetization-prepared rapid acquisition gradient echo sequence to generate high-resolution anatomic data. [^{18}F]T807 PET data were spatially normalized to the MNI template brain using SPM2.

Data Analysis

DAT concentration in the putamen and caudate ROIs was evaluated using a backward elimination general linear model (GLM) regressed on the initial predictor pool: diagnostic group, age at imaging, education, putamen DAT (for the caudate analyses), duration of motor symptoms, levodopa-equivalent dose and the interaction of diagnosis with each of the other predictors. The cutoff p value for removal from the model was 0.01. A covariate of caudate volume and its interaction with diagnosis were included when caudate DAT concentration was the dependent variable. Tukey post hoc tests were performed as required to follow up significant diagnostic main effects. We assessed the relation of DAT concentration to CDR-SB using GLM analyses with backward elimination ($p > 0.01$ for removal from the model), with a pool of predictors that initially included diagnostic group, DAT concentration in the selected ROIs, interaction of diagnosis with ROIs, caudate volume, age, education, duration of motor symptoms and levodopa-equivalent dose.

Precuneus PiB retention (DVR) was compared across the diagnostic groups (PD, PD-MCI, PDD, DLB and HCS) using a backward elimination GLM with PiB as the dependent variable and with an initial pool of predictor variables which included diagnostic group, age at imaging and interactions of diagnosis with age. Cutoff p values for removal from the model were set at 0.05. Tukey-adjusted post hoc tests were performed where required to follow up significant main effects.

For longitudinal PiB analyses, longitudinal change in the CDR-SB was assessed with mixed random/fixed coefficient longitudinal regression models. We conducted backward elimination of fixed terms, which included baseline diagnosis (PD-nl/PD-MCI) and its interaction with time, PiB DVR and its interaction with time, gender, years of education, baseline age and baseline duration of motor symptoms. The relation of PiB DVR to time to transition to a more severe diagnosis was assessed with Cox proportional hazards regression models containing the predictors of PiB DVR, baseline diagnosis and its interaction with PiB, baseline age/duration, years of education and gender. Earliest transitions from PD-nl to PD-MCI (or PDD) and from PD-MCI to PDD were both included in the analysis. PD subjects either remained stable in their diagnosis across time (considered 'censored' observations in the model) or transitioned to a more severe diagnosis. The assumption of proportional hazards was checked and verified.

SAS (version 9.3) and JMP Pro software were used for analyses and graphs.

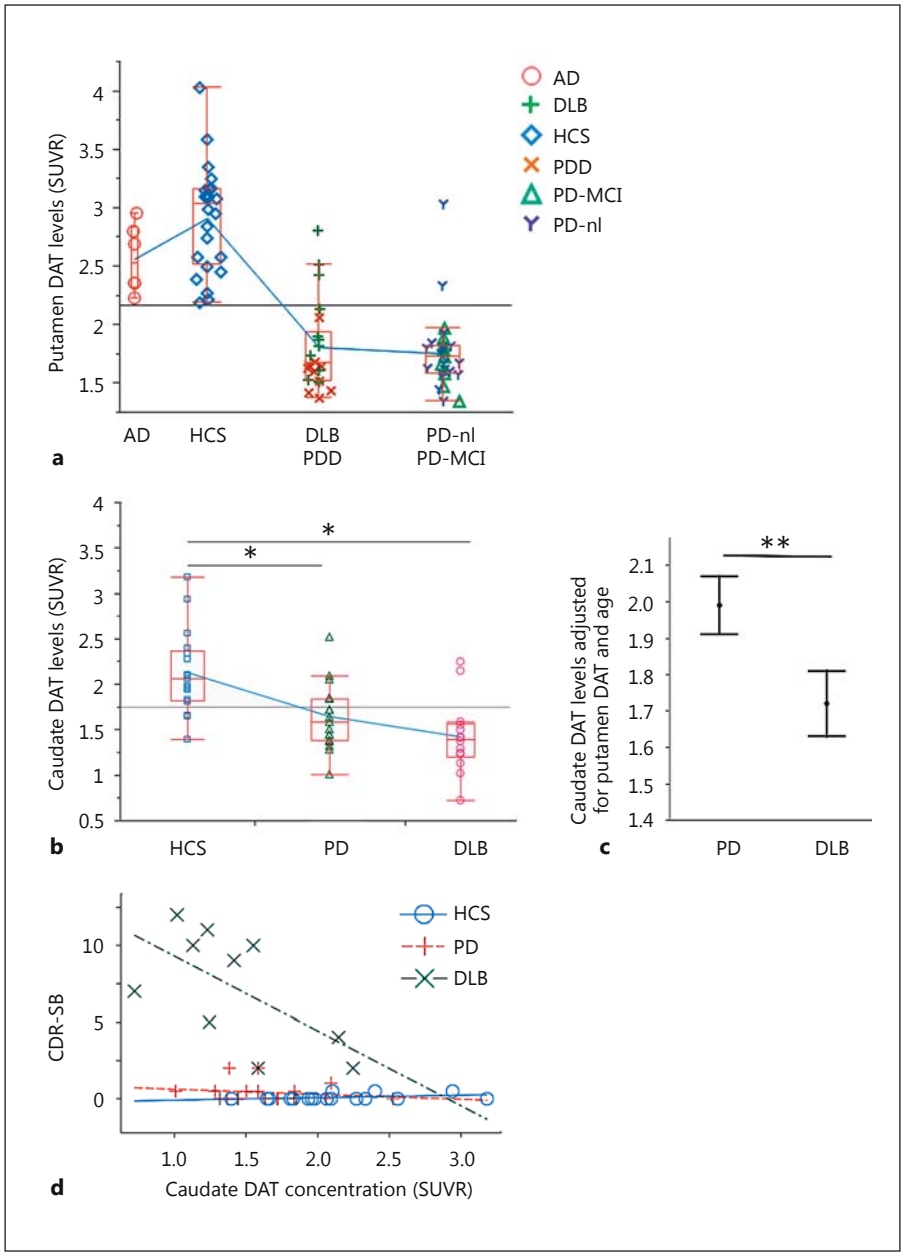

Fig. 1. Altropane imaging in DLB and PD. **a** Putamen DAT levels differentiate DLB, PDD, and nondemented PD from AD and HCS. Putamen DAT levels in the DLB/PDD and the nondemented PD groups were similar to each other and lower than the putamen DAT levels of AD and HCS ($p < 0.0001$ for each comparison). **b**, **c** Relative caudate DAT concentration differentiates DLB from nondemented PD. **b** Caudate DAT levels were lower in DLB and nondemented PD than in HCS (DLB vs. HCS, * $p < 0.0003$; PD vs. HCS, * $p < 0.0003$). **c** Adjusting for putamen DAT concentration and age, caudate DAT concentration in DLB was lower than in nondemented PD (** $p < 0.041$). **d** Caudate DAT concentration relates to cognitive function in DLB but not in nondemented PD. Adjusting for age, duration of motor symptoms and putamen DAT concentration, higher CDR-SB was associated with greater reduction in DAT concentration in DLB ($R^2 = 0.84$, $p < 0.0001$ for model). Note that a similar decline in caudate DAT concentration in nondemented PD was not associated with a similar impairment on the CDR-SB ($p = 0.0008$ for interaction between DAT concentration and diagnosis).

Results

DAT Imaging

Putamen DAT concentration was significantly lower in the Lewy body dementia cases (DLB and PDD) than in AD and HCS (each comparison, $p < 0.0001$, GLM; fig. 1a). In addition, caudate DAT concentration, assessed with Freesurfer, was also lower in DLB and in PD than in HCS (each comparison, $p < 0.0003$; fig. 1b). Adjusting for age and for putamen DAT concentration, as a measure of severity of motor system impairment, caudate DAT concentration was significantly lower in DLB than in PD ($p < 0.041$; fig. 1c). These data confirm the value of DAT imaging with altropane both to differentiate DLB and PDD from AD and to distinguish DLB from PD.

We also examined the relation of caudate DAT concentration to cognitive function in DLB. Adjusting for age, duration of motor symptoms and putamen DAT concentration, greater functional impairment in DLB, measured with the CDR-SB, was associated with greater

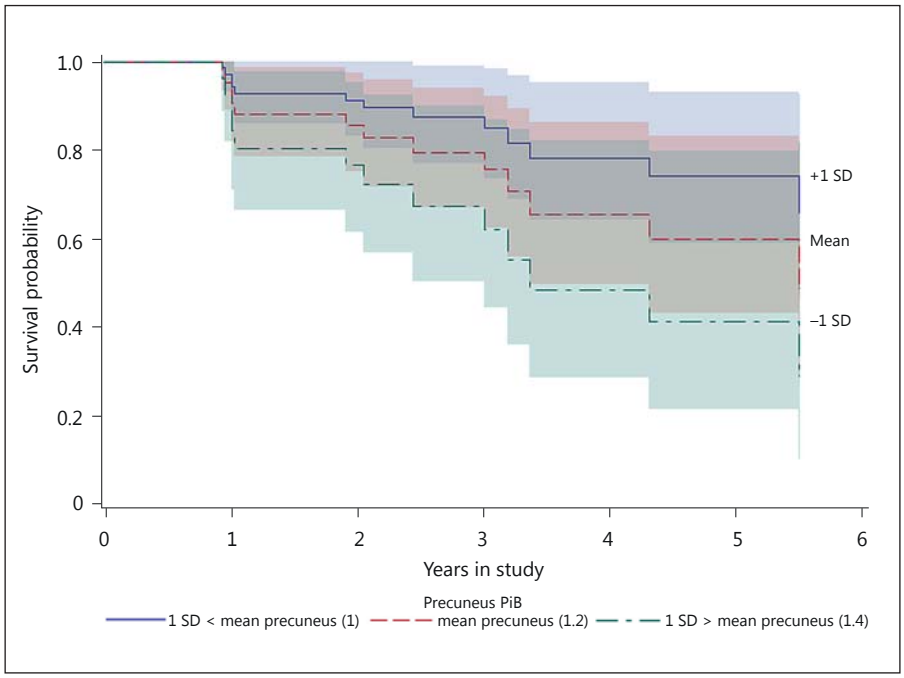

Fig. 2. Survivor functions with 95% confidence limits: greater amyloid burden in PD, measured as PiB retention in the precuneus, is associated with a faster transition to a severer cognitive diagnosis. PD-nl and PD-MCI groups were pooled for this analysis, and transitions from PD-nl to PD-MCI or PDD, and from PD-MCI to PDD, were evaluated (p = 0.008; Cox regression). The survival probability is shown for precuneus PiB DVR of 1 standard deviation below (1) and above (1.4) the mean (1.2).

reduction in DAT concentration (R^2 = 0.84, p < 0.0001 for model; fig. 1d). In contrast, a similar reduction of caudate DAT concentration in PD was not associated with impairment in the CDR-SB (p = 0.0008 for interaction between DAT concentration and diagnosis). Thus, progressive dopamine denervation of the caudate appears to contribute to cognitive impairment in DLB but is not sufficient for cognitive impairment in PD.

Amyloid Imaging

Cortical amyloid burden measured with [^{11}C]PiB was higher in DLB than in HCS, PD or PDD (p < 0.0001 for model, p < 0.002 for each group contrast). Even so, specific cortical PiB retention was present in many PD-nl, PD-MCI and PDD subjects, as well as in approximately 30% of HCS.

We have continued to follow the PD cohort with annual neuropsychological evaluation and neurological examinations, in order to relate amyloid burden to the course of cognitive impairment in PD and DLB. As we first described in 2013 [11] and have now extended, higher PiB uptake predicted a faster conversion of diagnosis from PD-nl to PD-MCI/PDD (n = 10/35) and PD-MCI to PDD (n = 5/11; p = 0.008; Cox regression; fig. 2). This corresponds to a hazard of conversion of 15.0 per unit PiB (DVR). In addition, higher PiB retention significantly related to a worsening CDR-SB score for subjects with PD-MCI or PDD (p = 0.0179; mixed random/fixed longitudinal model). These data confirm that amyloid burden is a risk factor for dementia in PD.

[^{18}F]T807 PET Imaging

We have begun [^{18}F]T807 PET acquisition in subjects clinically diagnosed with PD, PDD, DLB and the parkinsonian tauopathies PSP and cortical basal ganglionic degeneration. In our preliminary experience in nondemented PD cases, [^{18}F]T807 uptake is increased in subjects with MCI. In addition, in PSP, the distribution of [^{18}F]T807 appears to correspond to the pattern of pathology, with high levels of [^{18}F]T807 binding in the globus pallidus and other affected deep gray structures. Greater sample sizes will be required to confirm these preliminary observations and determine whether [^{18}F]T807 binding relates to amyloid burden and to cognitive impairment in PD and differentiates the synucleinopathies from the parkinsonian tauopathies.

Discussion

The use of PET imaging to evaluate molecular neuropathologies in living patients with PD and DLB continues to provide new insights into these disorders. Consistent with prior reports with other DAT imaging ligands,

we find that reduction of putamen DAT concentration in DLB, measured with altropane, appears to provide a useful distinction from AD, where putamen DAT is relatively preserved. Furthermore, the relative loss of caudate DAT provides a means to differentiate DLB from PD. The observation that loss of caudate DAT concentration, after adjusting for putamen DAT concentration, is associated with cognitive impairment in DLB but not in PD suggests that additional pathological processes, such as α-synuclein aggregation and the presence of copathologies, make DLB brains susceptible to loss of caudate dopamine.

One such copathology, deposition of β-amyloid, is well evaluated with PiB PET imaging. In our experience and that of other studies [9], cortical amyloid deposition is common and is often high in DLB, while cortical amyloid burden is common but often lower in PDD and PD. Nonetheless, cortical amyloid deposits are associated with a significant risk for cognitive decline in PD, in a dose-dependent manner. Thus, amyloid copathology is common and deleterious in both DLB and PD. These data suggest that treatments under development for AD that target β-amyloid 42 are likely to have clinical value in DLB and PD as well.

As yet, our preliminary experience with [^{18}F]T807 supports its potential as a marker of cognitive impairment in PD and as an imaging method to differentiate PD and DLB from PSP and cortical basal ganglionic degeneration. We continue to evaluate these hypotheses.

In conclusion, DAT and amyloid imaging offer a powerful approach to diagnose DLB and PDD and to explore the molecular basis of dementia in these disorders. [^{18}F] T807 may prove to be a useful additional imaging modality for these purposes.

Acknowledgments

We thank Randy Buckner for providing the altropane data for the healthy control group. We thank Alex Becker and Aaron Schultz for assistance with data analysis. This research was supported by the Michael J. Fox Foundation (to S.N.G. and J.H.G.), National Alzheimer's Coordinating Center Collaborative Project 5 U01 AG016976-11 (to S.N.G., K.A.J. and J.H.G.), the National Institute of Neurological Disorders and Stroke (to S.N.G., K.A.J. and J.H.G.; to K.A.J. alone), the National Institute on Aging (to K.A.J.), the Alzheimer's Disease Association (to K.A.J.), the National Parkinson Foundation (to S.N.G., K.A.J. and J.H.G.), the Harvard Center for Neurodegeneration and Repair Pilot grant (to S.N.G.) and the Caja Madrid Foundation (to M.M.).

Disclosure Statement

Dr. Gomperts has nothing to disclose.

References

1 McKeith IG, Dickson DW, Lowe J, Emre M, O'Brien JT, Feldman H, Cummings J, Duda JE, Lippa C, Perry EK, Aarsland D, Arai H, Ballard CG, Boeve B, Burn DJ, Costa D, Del Ser T, Dubois B, Galasko D, Gauthier S, Goetz CG, Gomez-Tortosa E, Halliday G, Hansen LA, Hardy J, Iwatsubo T, Kalaria RN, Kaufer D, Kenny RA, Korczyn A, Kosaka K, Lee VM, Lees A, Litvan I, Londos E, Lopez OL, et al: Diagnosis and management of dementia with Lewy bodies: third report of the DLB Consortium. Neurology 2005;65:1863–1872.

2 Lippa CF, Duda JE, Grossman M, Hurtig HI, Aarsland D, Boeve BF, Brooks DJ, Dickson DW, Dubois B, Emre M, Fahn S, Farmer JM, Galasko D, Galvin JE, Goetz CG, Growdon JH, Gwinn-Hardy KA, Hardy J, Heutink P, Iwatsubo T, Kosaka K, Lee VM, Leverenz JB, Masliah E, McKeith IG, Nussbaum RL, Olanow CW, Ravina BM, Singleton AB, Tanner CM, Trojanowski JQ, Wszolek ZK; DLB/PDD Working Group: DLB and PDD boundary issues: diagnosis, treatment, molecular pathology, and biomarkers. Neurology 2007;68:812–819.

3 Huang Y, Halliday G: Can we clinically diagnose dementia with Lewy bodies yet? Transl Neurodegener 2013;2:4.

4 Politis M: Neuroimaging in Parkinson disease: from research setting to clinical practice. Nat Rev Neurol 2014;10:708–722.

5 Fischman AJ, Bonab AA, Babich JW, Livni E, Alpert NM, Meltzer PC, Madras BK: [(11)C, (127)I] Altropane: a highly selective ligand for PET imaging of dopamine transporter sites. Synapse 2001;39:332–342.

6 Marquie M, Locascio JJ, Rentz DM, Becker JA, Hedden T, Johnson KA, Growdon JH, Gomperts SN: Striatal and extrastriatal dopamine transporter levels relate to cognition in Lewy body diseases: an (11)C altropane positron emission tomography study. Alzheimers Res Ther 2014;6:52.

7 Harding AJ, Halliday GM: Cortical Lewy body pathology in the diagnosis of dementia. Acta Neuropathol 2001;102:355–363.

8 Howlett DR, Whitfield D, Johnson M, Attems J, O'Brien JT, Aarsland D, Lai MK, Lee JH, Chen C, Ballard C, Hortobágyi T, Francis PT: Regional multiple pathology scores are associated with cognitive decline in Lewy body dementias. Brain Pathol 2015;25:401–408.

9 Gomperts SN: Imaging the role of amyloid in PD dementia and dementia with Lewy bodies. Curr Neurol Neurosci Rep 2014;14:472.

10 Andersson M, Zetterberg H, Minthon L, Blennow K, Londos E: The cognitive profile and CSF biomarkers in dementia with Lewy bodies and Parkinson's disease dementia. Int J Geriatr Psychiatry 2011;26:100–105.

11 Gomperts SN, Marquie-Sayagues M, Locascio JJ, Rentz D, Santarlasci AL, Johnson KA, Growdon JH: Amyloid is linked to cognitive decline in patients with Parkinson disease without dementia. Neurology 2013;80:85–91.

12 Siderowf A, Xie SX, Hurtig H, Weintraub D, Duda J, Chen-Plotkin A, Shaw LM, Van Deerlin V, Trojanowski JQ, Clark C: CSF amyloid {beta} 1–42 predicts cognitive decline in Parkinson disease. Neurology 2010;75:1055–1061.

13 Villemagne VL, Fodero-Tavoletti MT, Masters CL, Rowe CC: Tau imaging: early progress and future directions. Lancet Neurol 2015;14:114–124.

14 Chien DT, Bahri S, Szardenings AK, Walsh JC, Mu F, Su MY, Shankle WR, Elizarov A, Kolb HC: Early clinical PET imaging results with the novel PHF-tau radioligand [F-18]-T807. J Alzheimers Dis 2013;34:457–468.
15 Hughes AJ, Daniel SE, Blankson S, Lees AJ: A clinicopathologic study of 100 cases of Parkinson's disease. Arch Neurol 1993;50:140–148.
16 Litvan I, Aarsland D, Adler CH, Goldman JG, Kulisevsky J, Mollenhauer B, Rodriguez-Oroz MC, Tröster AI, Weintraub D: MDS Task Force on mild cognitive impairment in Parkinson's disease: critical review of PD-MCI. Mov Disord 2011;26:1814–1824.
17 Emre M, Aarsland D, Brown R, Burn DJ, Duyckaerts C, Mizuno Y, Broe GA, Cummings J, Dickson DW, Gauthier S, Goldman J, Goetz C, Korczyn A, Lees A, Levy R, Litvan I, McKeith I, Olanow W, Poewe W, Quinn N, Sampaio C, Tolosa E, Dubois B: Clinical diagnostic criteria for dementia associated with Parkinson's disease. Mov Disord 2007;22:1689–1707.
18 Gomperts SN, Locascio JJ, Marquie-Sayagues M, Santarlasci AL, Rentz D, Maye J, Johnson KA, Growdon JH: Brain amyloid and cognition in Lewy body diseases. Mov Disord 2012;27:965–973.
19 Thie JA: Understanding the standardized uptake value, its methods, and implications for usage. J Nucl Med 2004;45:1431–1434.
20 Lewis DA, Melchitzky DS, Sesack SR, Whitehead RE, Auh S, Sampson A: Dopamine transporter immunoreactivity in monkey cerebral cortex: regional, laminar, and ultrastructural localization. J Comp Neurol 2001;432:119–136.
21 Becker JA, Hedden T, Carmasin J, Maye J, Rentz DM, Putcha D, Fischl B, Greve DN, Marshall GA, Salloway S, et al: Amyloid-beta associated cortical thinning in clinically normal elderly. Ann Neurol 2011;69:1032–1042.
22 Logan J, Fowler JS, Volkow ND, Wang GJ, Ding YS, Alexoff DL: Distribution volume ratios without blood sampling from graphical analysis of PET data. J Cereb Blood Flow Metab 1996;16:834–840.
23 Lopresti BJ, Klunk WE, Mathis CA, Hoge JA, Ziolko SK, Lu X, Meltzer CC, Schimmel K, Tsopelas ND, DeKosky ST, Price JC: Simplified quantification of Pittsburgh compound B amyloid imaging PET studies: a comparative analysis. J Nucl Med 2005;46:1959–1972.